

## Reentrant behavior of the phase stiffness in Josephson junction arrays

Luca Capriotti,<sup>1</sup> Alessandro Cuccoli,<sup>2,3</sup> Andrea Fubini,<sup>2,3</sup> Valerio Tognetti,<sup>2,3</sup> and Ruggero Vaia<sup>4,3</sup><sup>1</sup>Kavli Institute for Theoretical Physics, University of California, Santa Barbara, CA 93106, USA<sup>2</sup>Dipartimento di Fisica dell'Università di Firenze – via G. Sansone 1, I-50019 Sesto Fiorentino (FI), Italy<sup>3</sup>Istituto Nazionale per la Fisica della Materia – U.d.R. Firenze – via G. Sansone 1, I-50019 Sesto Fiorentino (FI), Italy<sup>4</sup>Istituto di Fisica Applicata ‘Nello Carrara’ del Consiglio Nazionale delle Ricerche,  
via Madonna del Piano, I-50019 Sesto Fiorentino (FI), Italy

(Dated: April 14, 2024)

The phase diagram of a 2D Josephson junction array with large substrate resistance, described by a quantum XY model, is studied by means of Fourier path-integral Monte Carlo. A genuine Berezinskii-Kosterlitz-Thouless transition is found up to a threshold value  $g^2$  of the quantum coupling, beyond which no phase coherence is established. Slightly below  $g^2$  the phase stiffness shows a reentrant behavior with temperature, in connection with a low-temperature disappearance of the superconducting phase, driven by strong nonlinear quantum fluctuations.

Two-dimensional Josephson junction arrays (JJA) are among the best experimental realizations of a model belonging to the XY universality class and offer the possibility of controlling and studying a variety of phenomena related to both the dynamics and the thermodynamics of vortices. In these systems a Berezinskii-Kosterlitz-Thouless (BKT) transition [1] separates the superconducting (SC) and the normal (N) state, the latter displaying no phase coherence [2]. For a nanoscale size of the junctions a new interesting feature shows up in the JJA, namely the quantum fluctuations of the superconducting phases. These are caused by the non-negligible energy cost of charge transfer between SC islands, a consequence of the small capacitances involved and the fact that phase and charge are canonically conjugated variables. A relevant effect is the progressive reduction of the SC-N transition temperature. Recently, fabricated arrays of nanosized junctions, both unshunted [3] and shunted [4], have given the opportunity to experimentally approach the quantum (zero temperature) phase transition.

However the mechanism of suppression of the BKT in the neighborhood of the quantum critical point and its connection with the observed reentrance of the array resistance as function of the temperature is not yet clear [2, 3, 5]. In this letter we study the SC-N phase diagram by means of path-integral Monte Carlo (PIMC) [6] simulations focusing the attention on the region of strong quantum fluctuations, in order to investigate their role in suppressing the BKT transition.

We describe the JJA on the square lattice by a quantum XY model with the following action

$$S[\varphi] = \int_0^{\beta} du \sum_{ij} \frac{\sim^2 C_{ij}}{8e^2} \dot{\varphi}_i(u) \dot{\varphi}_j(u) - E_J \sum_{\langle ij \rangle} \cos \varphi_{ij}(u); \quad (1)$$

where  $\varphi_{ij} = \varphi_i - \varphi_j$  is the phase difference between the  $i$ th and the  $j$ th neighboring superconducting islands. We assume the presence of weak Ohmic dissipation due to

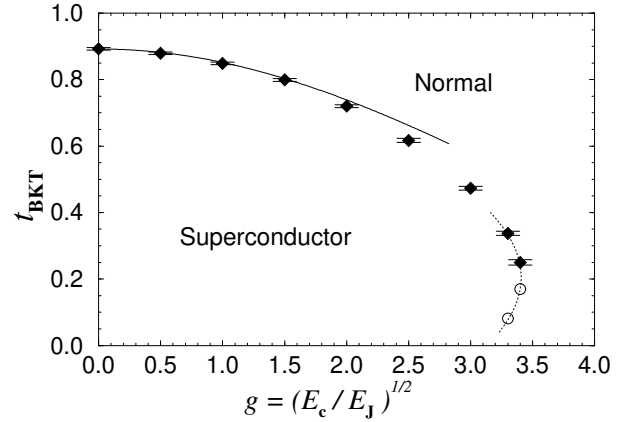


FIG. 1: Phase diagram for a JJA on a square lattice in the limit  $R_s \rightarrow R_0 = h/(2e)^2$  with  $\beta = 10^{-2}$ . The symbols are our PIMC results; the solid line reports the semiclassical result of the PQSCHA [8]. The dashed line is a guide for the eye (see text).

small currents flowing to the substrate or through shunt resistances [4], which reflects into the prescription to consider the phase as an extended variable [2]. The capacitance matrix reads  $C_{ij} = C_0 \delta_{ij} + (z_{ij} / d) C$ , where  $C_0 = C$  [7] and  $C$  are, respectively, the self- and mutual capacitances of the islands, and  $d$  runs over the vector displacements of the  $z = 4$  nearest-neighbors.

The quantum dynamics of this system is ruled by the competition between the Coulomb interaction of Cooper pairs, described by the kinetic term, and the Josephson coupling represented by the cosine term. The quantum fluctuations are therefore ruled by the quantum coupling parameter  $g = E_c / E_J$ , where  $E_c = (2e)^2 / 2C$  is the characteristic charging energy (for  $\beta = 1$ ). It is also convenient to use the dimensionless temperature  $t = k_B T / E_J$ . In our model Eq. (1) we did not include any explicit dissipation term, as dissipative effects are negligible provided that the shunt resistance  $R_s \rightarrow R_0 = h/(2e)^2$  is the quantum resistance; for

smaller  $R_s$  the Caldeira-Leggett term can be added to the action [1] [2, 8], resulting in a decrease of quantum fluctuations.

Fig. 1 displays our resulting phase diagram together with the semiclassical results valid at low coupling [8]. At high temperature, the system is in the N state with exponentially decaying phase correlations,  $\langle \psi_i^\dagger \psi_j \rangle$ , and vanishing phase stiffness. By lowering  $t$ , for  $g < g^2 \approx 3.4$ , the system undergoes a BKT phase transition at  $t_{\text{BKT}}(g)$  to a SC state with power-law decaying phase correlations and finite stiffness. When  $g$  is small enough (semiclassical regime), the critical temperature smoothly decreases by increasing  $g$  and it is in remarkable agreement with the predictions of the pure-quantum self-consistent harmonic approximation (PQ-SCHA) [8]. For larger  $g$  (but still  $g < g^2$ ) the semiclassical treatment becomes less accurate and the curve  $t_{\text{BKT}}(g)$  shows a steeper reduction, but the SC-N transition still obeys the standard BKT scaling behavior. Finally, for  $g > g^2$  a strong quantum coupling regime with no sign of a SC phase is found. Surprisingly, the BKT critical temperature does not scale down to zero by increasing  $g$  (i.e.,  $t_{\text{BKT}}(g^2) \neq 0$ ): by reducing the temperature in the region  $3.2 < g < g^2$ , phase coherence is first established, as a result of the quenching of thermal fluctuations, and then destroyed again due to a dramatic enhancement of quantum fluctuations near  $t = 0$ . This is evidenced by a reentrant behavior of the stiffness of the system, which vanishes at low and high  $t$  and it is finite at intermediate temperatures. The open symbols in Fig. 1 mark the transition between the finite and zero stiffness region when  $t$  is lowered.

These results are obtained using PIMC simulations on  $L \times L$  lattices (up to  $L = 96$ ) with periodic boundary conditions. Thermodynamic averages are obtained by MC sampling of the partition function after discretization of the Euclidean time  $\tau \in [0; \beta]$  in  $P$  slices  $\tau_P$ , where  $P$  is the Trotter number, using the standard Metropolis algorithm. The actual sampling is made on imaginary-time Fourier transformed variables using the same algorithm developed in Ref. 6: thanks to the fact that the move amplitudes are independently chosen and dynamically adjusted for each Fourier component, this procedure ensures to efficiently reproduce the strong quantum fluctuations of the paths in the region of high quantum coupling  $g$ . Indeed, test simulations with the standard PIMC algorithm showed serious problems of ergodicity, though eventually giving the same results. The autocorrelation times has been reduced by an over-relaxation algorithm [9] over the zero-frequency mode.

A very sensitive method to determine the critical temperature is provided by the scaling law of the helicity modulus  $\Upsilon_L$ , a quantity proportional to the phase stiffness. Measures the response of the system to the application of a twist  $k_0$  to the boundary conditions along

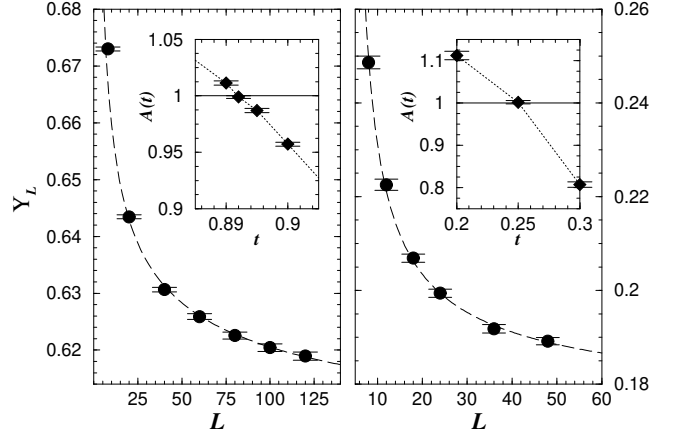


FIG. 2: Size scaling of the helicity modulus  $\Upsilon_L$  at the transition temperature. Symbols are PIMC data and the dashed-lines are the one-parameter fit with Eq. (3). Left panel:  $g = 0$  and  $t = 0.892$  [ $L_0 = 0.456(6)$ ]; right panel:  $g = 3.4$  and  $t = 0.25$  [ $L_0 = 3.32(3)$ ]. The insets show  $A(t)$  for different temperatures, using the two-parameter fit (see text).

a fixed direction,

$$\Upsilon_L = \frac{1}{E_J} \frac{\partial^2 F}{\partial k_0^2} \Big|_{k_0=0}; \quad (2)$$

where  $F$  is the free energy. By derivation of the discretized path-integral expression of the partition function, the PIMC estimator for  $\Upsilon_L$  is easily obtained, in analogy to that of Ref. [10]. Kosterlitz's renormalization group equations provide the critical scaling law for the finite-size helicity modulus  $\Upsilon_L$ :

$$\frac{\Upsilon_L(t_{\text{BKT}})}{t_{\text{BKT}}} = \frac{2}{L_0} \left( 1 + \frac{1}{2 \log(L/L_0)} \right); \quad (3)$$

where  $L_0$  is a non-universal constant. Following Ref. [11], the critical temperature can be found by fitting  $\Upsilon_L(t) \sim t$  vs  $L$  for several temperatures according to Eq. (3) with a further multiplicative fitting parameter  $A(t)$ . In this way, the critical point can be determined by searching the temperature such that  $A(t_{\text{BKT}}) = 1$ , as illustrated in Fig 2. This is the technique we used to get the filled symbols in Fig. 1. Using this procedure the critical temperature can be determined with excellent precision. For instance in the classical case we get  $t_{\text{BKT}}(g=0) = 0.892(2)$ , in very good agreement with the most accurate results from classical simulations [12]. Also in the regime of strong quantum coupling,  $g = 3.4$ , the PIMC data for  $\Upsilon_L(t_{\text{BKT}} = 0.25)$  are very well fitted by Eq. (3), as shown in Fig. 3. Moreover, this figure points out the sensitivity of this method to identify  $t_{\text{BKT}}$ : at temperature higher (lower) than the critical one the helicity modulus decreases (increases) much faster with  $L$  than  $\Upsilon_L(t_{\text{BKT}})$ . At higher values of the quantum coupling,  $g > g^2$ , the helicity modulus scales to zero with  $L \rightarrow 1$  and  $P \rightarrow 1$  at any temperature.

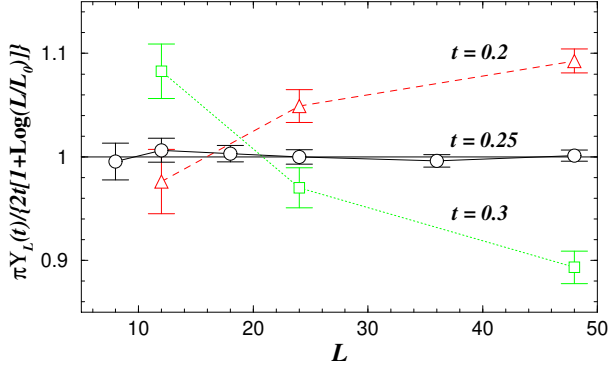


FIG. 3: Helicity modulus  $Y_L$  divided by the best fit with the expression (3) for  $g = 3.4$  and different temperatures: 0.2, 0.25, and 0.3, respectively.

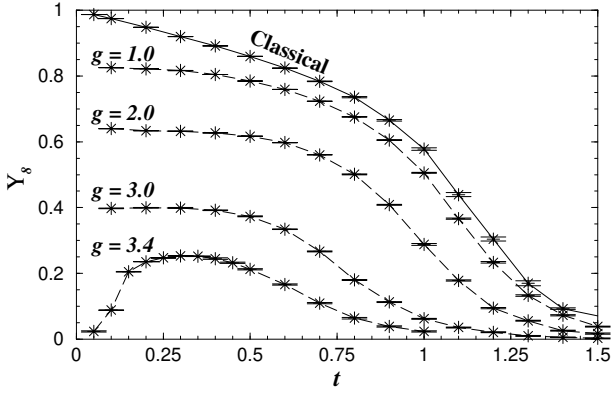


FIG. 4: Temperature behavior of the helicity modulus  $Y_8(t)$  on a  $8 \times 8$  lattice, for different values of  $g$ . The data are results from the Trotter extrapolation.

At variance with the standard BKT theory, in the regime of strong quantum fluctuations we find a range of coupling values,  $3.2 \lesssim g \lesssim g^2$ , in which the helicity modulus displays a non-monotonic temperature behavior. In Fig. 4,  $Y_L(t)$  is plotted for different values of  $g$  on the  $8 \times 8$  cluster: up to  $g = 3.0$  it shows a monotonic behavior similar to the classical case, where thermal fluctuations drive the suppression of the phase stiffness. In contrast, for  $g = 3.4$ , the helicity modulus is suppressed at low temperature, then it increases up to  $t \approx 0.2$ ; for further increasing temperature it recovers the classical-like behavior and a standard BKT transition can still be located at  $t \approx 0.25$  (Figs. 2 and 3). A reentrance of the phase stiffness was found for a related model in Ref. [10], but the authors concluded that the low temperature drop of the helicity modulus was probably due to having a finite Trotter number. In order to ascertain this point, we have performed systematic extrapolations in the Trotter number and in the lattice size, as illustrated in Figs. 5 and 6 for  $g = 3.4$ . We have found no sign of anomalies in the finite- $P$  behavior: the extrapolations in the Trotter number appear to be well-

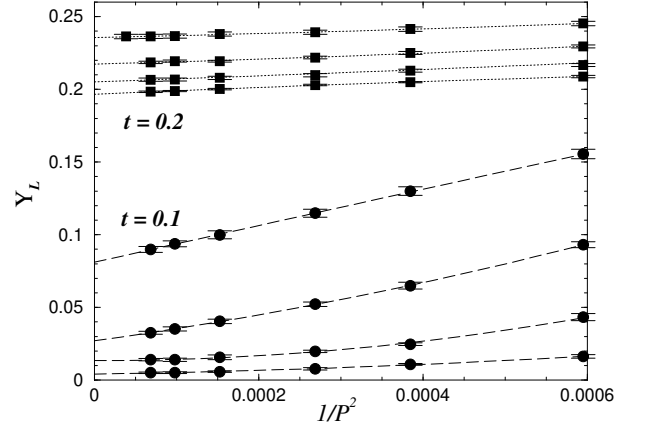


FIG. 5: Trotter-number extrapolation of  $Y_L$  for  $g = 3.4$ . Two series of data for  $t = 0.1$  (●) and  $0.2$  (■) are reported, for four different lattice sizes: from the top to the bottom  $L = 8; 10; 12; 14$ . The lines are weighted quadratic fits.

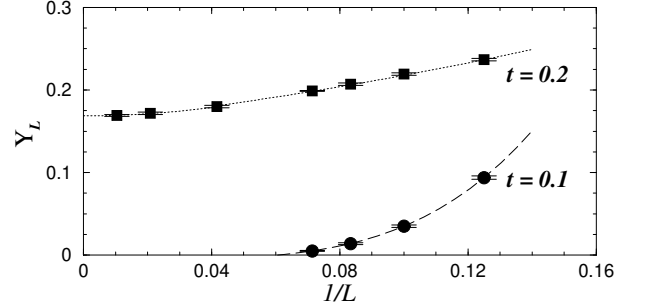


FIG. 6: Finite-size scaling of the helicity modulus  $Y_L$  for  $g = 3.4$  at fixed  $P = 101$ . The lines are guides for the eye.

behaved and already in the expected asymptotic regime  $O(1/P^2)$  [13], for  $P \gtrsim 60$  (Fig. 5). The extrapolation to infinite lattice size shown in Fig. 6 clearly indicates that  $Y_L$  scales to zero at  $t = 0.1$ , while it remains finite and sizeable at  $t = 0.2$ . Hence, the outcome of our analysis is opposite to that of Ref. [10], i.e., we conclude that the reentrant behavior of the helicity modulus is a genuine effect present in our model, rather than a finite-Trotter or finite-size artifact.

In order to understand the physical reasons of the reentrance observed in the phase stiffness, we have studied the following two quantities:

$$\cos \langle \theta'_{ij}(u) \rangle; \quad (4)$$

$$\langle \theta'^2_{ij} \rangle = \langle (\theta'_{ij}(u) - \langle \theta'_{ij}(u) \rangle)^2 \rangle; \quad (5)$$

with  $\langle \theta'_{ij} \rangle = (\int_0^{2\pi} \theta'_{ij}(u) du)^{1/2}$  and  $ij$  nearest-neighbor sites. The first quantity is a measure of the total (thermal and quantum) short-range fluctuations of the Josephson phase: in particular, it has a maximum where the overall fluctuation effect is weakest. The second quantity represents instead the "pure quantum" spread of the phase difference between two neighboring islands and has

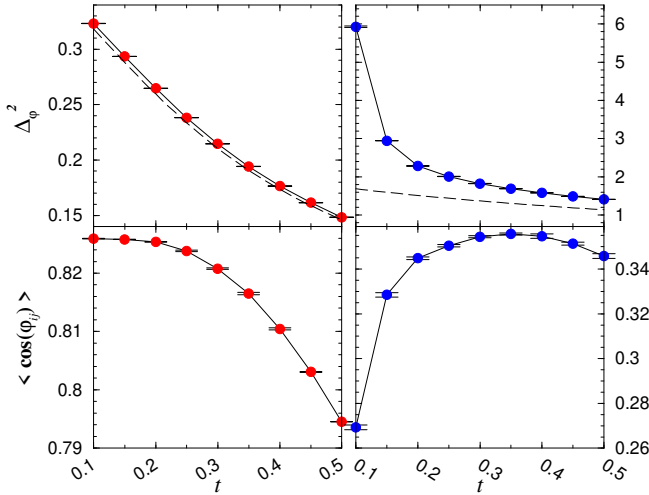


FIG. 7: Top panels:  $\Delta\phi^2$  vs  $t$ ; bottom panels:  $\langle \cos(\phi_{ij}) \rangle$  vs  $t$ . The quantum coupling is  $g = 1.0$  in the left panels and  $g = 3.4$  in the right panels. The circles are PIMC data and the dashed lines are PQSCHA results.

been recently studied in the single junction problem [14]; more precisely,  $\Delta\phi^2$  measures the fluctuations around the "static" value (i.e., the zero-frequency component of the Euclidean path), it is maximum at  $t = 0$  and tends to zero in the classical limit (i.e.,  $g \rightarrow \infty$ ).

The quantities (4) and (5) on a  $8 \times 8$  lattice are compared in Fig. 7 for two values of the quantum coupling, in the semiclassical ( $g = 1.0$ ) and in the extreme quantum ( $g = 3.4$ ) regime. In the first case  $\langle \cos(\phi_{ij}) \rangle$  decreases monotonically by increasing  $t$  and the pure-quantum phase spread  $\Delta\phi^2$  shows a semiclassical linear behavior which is correctly described by the PQSCHA. At variance with this, at  $g = 3.4$ , where the reentrance of  $\langle t \rangle$  is observed,  $\langle \cos(\phi_{ij}) \rangle$  displays a pronounced maximum at finite temperature. Besides the qualitative agreement with the mean-field prediction of Ref. [15], we find a much stronger enhancement of the maximum above the  $t = 0$  value. This remarkable finite- $t$  effect can be explained by looking at  $\Delta\phi^2$  ( $g = 3.4$ ) (Fig. 7, top-right panel). Its value is an order of magnitude higher than the one in the semiclassical approximation and, notably, it is strongly suppressed by temperature in a qualitatively different way from  $\Delta\phi^2$  ( $g = 1.0$ ): the pure-quantum contribution to the phase fluctuations measured by  $\Delta\phi^2$  decreases much faster than the linearly rising classical (thermal) one. Thus the interplay between strong quantum coupling and temperature turns out in a finite- $t$  minimum of the total fluctuations of the Josephson phase. This single-junction effect in a definite interval of the quantum coupling ( $3.2 \lesssim g \lesssim 3.4$ ) is so effective to drive the reentrance of the phase stiffness.

As for this low-temperature transition, the open symbols in Fig. 1 represent the approximate location of the points  $(t; g)$  where  $\langle t \rangle$  becomes zero within the error bars: in their neighborhood we did not find any BKT-like

scaling law. This fact opens two possible interpretations: (i) the transition does not belong to the XY universality class; (ii) it does, and in this case the control parameter is not the (renormalized) temperature, but a more involved function of both  $t$  and  $g$ . Further investigations are needed to answer this question.

In summary, we have studied a model for a JJA in the quantum fluctuation dominated regime. The BKT phase transition has been followed increasing the quantum coupling  $g$  up to a critical value  $g^2 \approx 3.4$  where  $t_{BKT} \approx 0.25$ ; above  $g^2$  no traces of BKT critical behavior have been observed. Remarkably, in the regime of strong quantum coupling ( $3.2 \lesssim g \lesssim 3.4$ ) phase coherence is established only in a finite range of temperatures, disappearing at higher  $T$ , with a genuine BKT transition to the normal state, and at lower  $T$ , due to a nonlinear quantum mechanical mechanism.

We acknowledge discussions with G. Falci, R. Fazio, M. Muser, T. Roscilde, and U. Weiss. We thank H. Baur and J. Wernz for assistance in using the MOSIX cluster in Stuttgart. L.C. was supported by NSF under Grant No. DMR-02-11166. This work was supported by the MIUR-COFIN 2002 program.

- 
- [1] V. L. Berezinskii, Sov. Phys. JEPT 32, 493 (1971); J. M. Kosterlitz and D. J. Thouless, J. Phys. C 6, 1181 (1973).
  - [2] R. Fazio and H. S. J. van der Zant, Phys. Rep. 355, 235 (2001).
  - [3] H. S. J. van der Zant, W. J. Elion, L. J. Geerligs and J. E. Mooij, Phys. Rev. B 54, 10081 (1996).
  - [4] Y. Takahide, R. Yagi, A. Kanda, Y. Otuka, and S. Kobayashi, Phys. Rev. Lett. 85, 1974 (2000).
  - [5] H. M. Jaeger, D. B. Haviland, B. G. Orr, and A. M. Goldman, Phys. Rev. B 40, 182 (1989).
  - [6] L. Capriotti, A. Cuccoli, A. Fubini, V. Tognetti, and R. Vaia, Europhys. Lett. 58, 155 (2002).
  - [7] The limits  $\beta \rightarrow 1$  and  $\beta \rightarrow \infty$  are more appropriate for the JJA and the granular films, respectively.
  - [8] A. Cuccoli, A. Fubini, V. Tognetti, and R. Vaia, Phys. Rev. B 61, 11289 (2000).
  - [9] F. R. Brown and T. J. Woch, Phys. Rev. Lett. 58, 2394 (1987).
  - [10] C. Rojas and J. V. Jose, Phys. Rev. B 54, 12361 (1996).
  - [11] K. Harada and N. Kawashima, J. Phys. Soc. Jpn. 67, 2768 (1998); A. Cuccoli, T. Roscilde, V. Tognetti, R. Vaia, and P. Vernocchi, Phys. Rev. B 67, 104414 (2003).
  - [12] P. Olsson, Phys. Rev. Lett. 73, 3339 (1994); M. Hasenbusch and K. Pinn, J. Phys. A 30, 63 (1997); S. G. Chung, Phys. Rev. B 60, 11761 (1999).
  - [13] M. Suzuki, Quantum Monte Carlo methods in equilibrium and nonequilibrium systems, ed. M. Suzuki (Springer-Verlag, Berlin, 1987).
  - [14] C. P. Herrero and A. Zaikin, Phys. Rev. B 65, 104516 (2002).
  - [15] P. Fazekas, B. Muhlischlegel, and Schroter, Z. Phys. B 57, 193 (1984).